RSC Advances

COMMUNICATION

View Article Online
View Journal | View Issue

Cite this: *RSC Adv.*, 2015, **5**, 803

Received 13th September 2014
Accepted 11th November 2014

DOI: 10.1039/c4ra10379c

www.rsc.org/advances

A rapid-response electrochromic device with significantly enhanced electrochromic performance†

Huiying Qu,‡[a] Hangchuan Zhang,‡[b] Na Li,[a] Zhongqiu Tong,[c] Jing Wang,[a] Jiupeng Zhao*[a] and Yao Li*[c]

A novel electrochromic device (ECD) was constructed with two same-material electrochromic layers deposited on indium-tin oxide (ITO)-coated glass substrates, a double-sided ITO-coated glass substrate, and a gel electrolyte. The device exhibited fast coloration/bleaching response and significantly enhanced optical modulation and coloration efficiency compared to traditional ECDs.

Optical properties of electrochromic (EC) materials can be changed reversibly and continuously by applying a low-voltage signal. Electrochromic devices (ECDs) composed of electrochromic materials, which allow the control of color cycles, have been extensively studied because of their wide applications in information displays,[1,2] rear-view mirrors,[3] smart windows,[4,5] and so on. To produce commercially viable ECDs, long-term cyclic stability, short response time, high coloration efficiency (CE), large optical modulation, and high initial transparency are the most important requirements. As an inorganic electrochromic material, tungsten trioxide (WO_3) has been most extensively studied because of its outstanding ion-transport properties and strong adhesion to the substrate.[6] Poly(3,4-ethylenedioxythiophene) (PEDOT), which is known for high optical contrast, and remarkable CE, has been regarded as the best conducting polymer available in terms of conductivity and stability.[7,8] Moreover, WO_3-based and PEDOT-based ECDs exhibit large optical modulation with a small charge insertion or extraction,[9,10] which are desirable advantages for a range of applications.

Compared with single-layered ECDs, it is well known that ECDs containing complementary electrochromic layers could further improve the EC performance such as optical modulation, CE, and cyclic stability.[11–13] As the two layers are always of different coloration types, such as ECDs composed of WO_3 and NiO,[12] where WO_3 is known as the typical cathodic coloration material and NiO as the typical anodic coloration material, two kinds of preparation methods are needed to obtain the complementary electrochromic layers. Therefore, a big challenge faced by scientists is to design novel ECDs with a simple preparation method and enhanced electrochromic performance. ECDs containing two same-material electrochromic layers seem to be promising alternatives to the complementary devices. In addition to high optical modulation and CE, like those of the complementary devices, the two electrochromic layers can be prepared by one method. Thus, this type of ECDs can be fabricated and controlled easily. However, to the best of our knowledge, there have been very few studies on ECDs containing two same-material electrochromic layers.

In this work, we attempted to design a novel ECD (referred to as NECD) using WO_3 and PEDOT as electrochromic materials. The WO_3 and PEDOT films were prepared by cathodic electrodeposition and electropolymerization, respectively. Each NECD was constructed with two sheets consisting of the same electrochromic material deposited on ITO-coated glass substrate, a double-sided ITO-coated glass substrate, and a gel electrolyte. Increased optical modulation and coloration efficiency were demonstrated by the resulting NECDs.

In a typical procedure, three-dimensionally ordered macroporous (3DOM) WO_3 films were prepared by cathodic electrodeposition in an ice-water-bath mixture of Na_2WO_4, 30% H_2O_2, and H_2SO_4 into polystyrene (PS) colloidal crystal templates grown on the ITO-coated glass substrates. As an additional example, the PEDOT films were obtained by electropolymerization using 1-butyl-3-methylimidazolium hexafluorophosphate ([Bmim]PF_6) containing 0.1 M 3,4-ethylenedioxythiophene (EDOT) on the exposed ITO-coated glass substrate (see the Experimental section in ESI†). The

[a]*School of Chemical Engineering and Technology, Harbin Institute of Technology, 150001, Harbin, China. E-mail: jpzhao@hit.edu.cn*

[b]*School of Science, Harbin Institute of Technology, 150001, Harbin, China*

[c]*Center for Composite Material, Harbin Institute of Technology, Harbin, China. E-mail: yaoli@hit.edu.cn; Fax: +86 451 86402345; Tel: +86 451 86402345*

† Electronic supplementary information (ESI) available: Electrodeposition of 3DOM WO_3 films; electropolymerization of PEDOT films; characterization procedures. See DOI: 10.1039/c4ra10379c

‡ These two authors contributed equally to this work.

double-sided ITO-coated glass substrate was then sandwiched between the electrochromic-material sides of the two ITO-coated glass substrates, and a gel electrolyte composed of a 1 M solution of $LiClO_4$ in propylene carbonate (PC) mixed with polymethylmethacrylate (PMMA) was introduced between the two electrodes by capillary action. Finally, the cell was sealed with epoxy, as shown schematically in Fig. 1. For comparison, a single-layered WO_3-ECD and a single-layered PEDOT-ECD were also prepared.

The characterization results of WO_3 and PEDOT films are summarized in Fig. 2. As can be seen in Fig. 2(a), owing to replication of the 3D ordered structures of the colloidal crystal templates, all WO_3 films grown directly on the ITO layers displayed highly periodic honeycomb structures with nanoscale walls throughout their entire volumes. The nanoscale walls could significantly decrease the diffusion length of Li^+ ions during electrochromic processes. Because of shrinkage during electrodeposition, the macroporous structures became slightly deformed. Such a hierarchical porous structure is expected to not only provide continuous pathways for electron transport, but also increase the number of possible intercalation sites. In the XRD pattern of the electrodeposited 3DOM WO_3 film (Fig. 2(b)), all peaks can be indexed as the planes of orthorhombic WO_3, which matches JCPDS card no. 81-1173.

The morphology of the PEDOT film, shown in Fig. 2(c), reveals that the relatively dense films prepared by electropolymerization had uniform thickness, and the thickness of the composite layer was dependent on the quantity of charge consumed during the preparation processes.

The *in situ* vibrational spectra of PEDOT were obtained by Raman spectroscopy. A number of well-defined bands assigned to PEDOT vibrations were found in the region of 500–2000 cm^{-1}, as shown in Fig. 2(d). The Raman spectrum of a dedoped PEDOT film recorded using 633 nm excitation shows features that are consistent with the positions and assignments of the bands for neutral PEDOT previously reported by Garreau *et al.*[14] using 1064 nm excitation. Owing to the vibrations of the neutral structure in PEDOT, the peaks at 1540, 1422, 1367, 1252, 1097, 988, 699, and 577 cm^{-1} are assigned to asymmetric $C_\alpha{=}C_\beta$ stretching, symmetric $C_\alpha{=}C_\beta(-O)$ stretching, $C_\beta{-}C_\beta$ stretching, $C_\alpha{-}C_{\alpha'}$ (inter-ring) stretching, C–O–C deformation, oxyethylene ring deformation, symmetric C–S–C deformation, and oxyethylene ring deformation, respectively.

Fig. 3 shows the electrochromic performances of the WO_3-ECD and WO_3-NECD. The optical transmittance spectra in Fig. 3(a) were measured at a wavelength of 700 nm with alternately applied potentials of +3 and −3 V for 20 s each; the corresponding photographs of the NECD fabricated from 3DOM WO_3 are shown in Fig. 3(d). The color of both the WO_3-ECD and WO_3-NECD switched between colorless (bleached state) and deep blue (colored state) with variations in the electric potential. From the transmittance spectra, it can be seen that the optical transmittance of the WO_3-ECD was 78% in the bleached

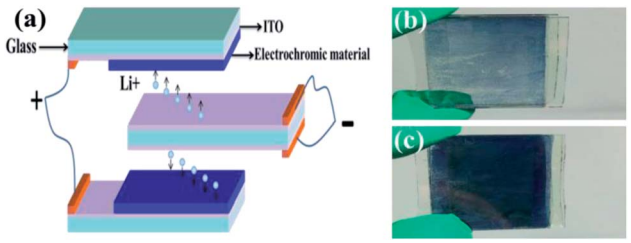

Fig. 1 (a) Schematic illustration of an NECD. Photos of a (b) colored and (c) bleached PEDOT-based NECD.

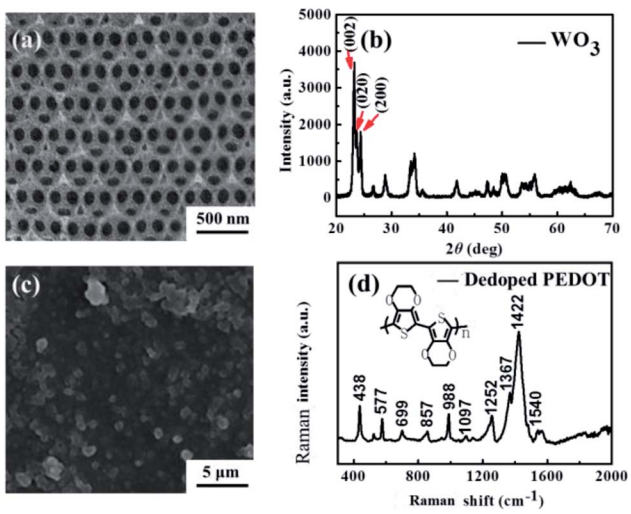

Fig. 2 Characterization of WO_3 and PEDOT films. (a) SEM image of the 3DOM WO_3 film with pore size of 440 nm. (b) XRD pattern of the 3DOM WO_3 film. (c) SEM image of the PEDOT film. (d) Raman spectrum of the as-synthesized PEDOT.

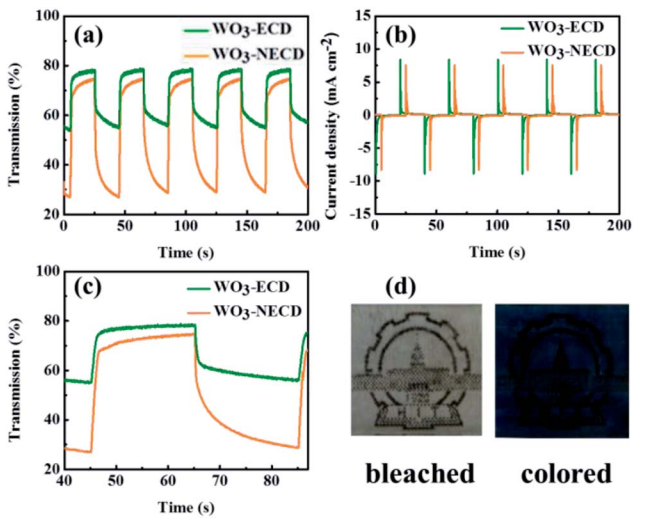

Fig. 3 Electrochromic performances of WO_3-ECD and WO_3-NECD. (a) Change in optical transmittance *versus* time. (b) Chronoamperometry curves obtained by applying a pulsed potential of ±3 V for 20 s for each state. (c) Corresponding transmittance variations and characteristic switching times between the colored and bleached states at a wavelength of 700 nm. (d) Photographs of the WO_3-NECD under potentials of +3 and −3 V, respectively.

state (3 V) and 50% in the colored state (−3 V), while the corresponding values for the WO_3-NECD were 75% and 27%, respectively. The transmittance variation of the WO_3-NECD reached about 48%, which is much higher than the variations of the WO_3-ECDs of 28% and 30%.[15] It can be ascribed to the synergetic effect of the two electrochromic layers.

The response time is defined as the time required to reach 90% of the final change in transmittance between the steady bleached and colored states. For the WO_3-NECD, the color-switching times from the colored state to the bleached state (t_b) and the reverse process (t_c) were 3.94 and 9.22 s, respectively, which are comparable with those of the WO_3-ECD (2.54 s and 7.56 s, respectively). Both the WO_3-NECD and WO_3-ECD demonstrated rapid response because of the 3DOM structure, which not only enhanced the crystallinity of the WO_3 film, thus improving the electron conductivity for effective electrochromic reactions, but also decreased Li^+ ions diffusion distances by maintaining a large active surface area and low mass-transport resistance.[16] It is noteworthy that the bleaching time is quite an outstanding value among those of tungsten-oxide-based ECDs in previous reports.[15,17–19]

Another important criterion for evaluation of the electrochromic performance of ECDs is CE, which represents the change in the optical density (OD) per unit charge density (Q/A), which is the change of the charge (Q) consumed per unit electrode area (A) during switching. It can be calculated according to the following equations:

$$CE = \Delta OD/Q$$

$$\Delta OD = \log(T_b/T_c)$$

where T_b and T_c refer to the bleached and colored transmittance, respectively, at a certain wavelength. The values of CE for the WO_3-ECD and WO_3-NECD were calculated from the current–time data shown in Fig. 3(b). The calculated CE value of the WO_3-NECD was 47.23 $cm^2\ C^{-1}$, which represents an approximate improvement of 82% compared with the CE value of the WO_3-ECD (25.94 $cm^2\ C^{-1}$), and the value is also superior to that of 35 $cm^2\ C^{-1}$.[15] The higher CE value indicates that the WO_3-NECD could provide large optical modulation with small changes in amount of inserted or extracted charge. This is a crucial parameter for practical devices since a lower charge-insertion or -extraction rate enhances the cyclic stability.

The structure we developed for the NECDs is powerful and adaptable, and it can be easily extended to fabricate other NECDs by simply choosing different EC materials (such as MoO_3, polyaniline (PANI), and viologen) and a suitable electrolyte. To demonstrate the versatility of the design, we also fabricated a PEDOT-NECD and obtained the corresponding electrochromic measurements.

Fig. 4 shows the electrochromic performances of the PEDOT-ECD and PEDOT-NECD. The color of the PEDOT-NECD switched between light blue (bleached state) and deep blue (colored state) with variations in the electric potential, while the color of the PEDOT-ECD was lighter in both states. From the

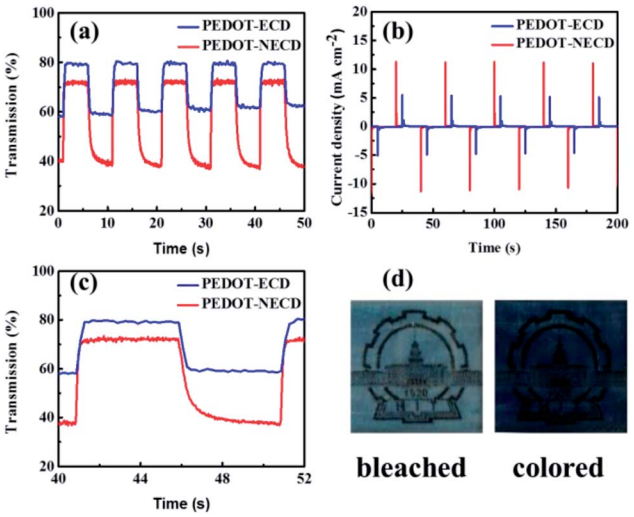

Fig. 4 Electrochromic performances of a PEDOT-ECD and a PEDOT-NECD. (a) Change in optical transmittance *versus* time. (b) Chronoamperometry curves by applying a pulsed potential of ±3 V for 10 s for each state. (c) Corresponding transmittance variations and characteristic switching times between the colored and bleached states at a wavelength of 580 nm. (d) Photographs of the PEDOT-NECD under potentials of +3 and −3 V.

transmittance spectra, it can be seen that the optical transmittance variation of the PEDOT-NECD at a wavelength of 580 nm reached about 58%, which is much higher than the PEDOT-ECD's variation of 17%, and that with variation of 30%.[20]

For the PEDOT-NECD, the response time was 0.20 s from the colored state to the bleached state and 1.20 s for the reverse process, which are comparable with the values obtained for the WO_3-ECD (0.36 s and 0.39 s, respectively). The CE values of the PEDOT-ECD and PEDOT-NECD were calculated from the current–time data shown in Fig. 4(b). The calculated CE value of PEDOT-NECD was 181.55 $cm^2\ C^{-1}$, which is a ~99% improvement compared with PEDOT-ECD's value (91.18 $cm^2\ C^{-1}$).

Conclusions

Rapid-response electrochromic devices based on two same-material electrochromic layers were fabricated with WO_3 and PEDOT. The uniform and well-adhered 3DOM WO_3 and PEDOT films were synthesized *via* electrodeposition and electropolymerization, respectively. The NECDs exhibited fast response time (t_b = 3.94 s and t_c = 9.22 s for WO_3; t_b = 3.05 s and t_c = 4.93 s for PEDOT), good cycling stability, and high initial transparency (75% for WO_3 and 69% for PEDOT). In addition, compared with the single-layered electrochromic device (CE: 25.94 $cm^2\ C^{-1}$ for WO_3 and 91.18 $cm^2\ C^{-1}$ for PEDOT; optical modulation: 28% at 700 nm for WO_3 and 17% at 580 nm for PEDOT), the NECDs demonstrated strikingly higher CE (47.23 $cm^2\ C^{-1}$ for WO_3 and 181.55 $cm^2\ C^{-1}$ for PEDOT) and larger optical modulation (48% at 700 nm for WO_3 and 58% at 580 nm for PEDOT), which can be ascribed to the synergetic effect of the two electrochromic layers. The excellent electrochromic performances combined with the easy fabrication

process make our devices highly suitable for applications in energy-saving smart windows and portable electronics.

Acknowledgements

We thank National Natural Science Foundation of China (no. 51010005, 91216123, 51174063), Natural Science Funds for Distinguished Young Scholar of Heilongjiang Province, The Natural Science Foundation of Heilongjiang Province (E201436) and the project of International Cooperation supported by Ministry of Science and Technology of China (2013DFR10630).

Notes and references

1 P. Periyat, N. Leyland, D. E. McCormack, J. Colreavy, D. Corr and S. C. Pillai, *J. Mater. Chem.*, 2010, **20**, 3650–3655.
2 C. G. Granqvist, *Sol. Energy Mater. Sol. Cells*, 2012, **99**, 1–13.
3 L. Han, L. Bai and S. Dong, *Chem. Commun.*, 2014, **50**, 802–804.
4 Z. Huang, C. Chen, C. Lv and S. Chen, *J. Alloys Compd.*, 2013, **564**, 158–161.
5 V. K. Thakur, G. Ding, J. Ma, P. S. Lee and X. Lu, *Adv. Mater.*, 2012, **24**, 4071–4096.
6 S. Adhikari and D. Sarkar, *RSC Adv.*, 2014, **4**, 20145–20153.
7 A. Elschner, S. Kirchmeyer, W. Lovenich, U. Merker and K. Reuter, *PEDOT: principles and applications of an intrinsically conductive polymer*, CRC Press, 2010.
8 I. F. Perepichka and D. F. Perepichka, *Handbook of thiophene-based materials: applications in organic electronics and photonics*, Wiley Online Library, 2009.
9 B. Kattouf, Y. Ein-Eli, A. Siegmann and G. L. Frey, *J. Mater. Chem. C*, 2013, **1**, 151–159.
10 H.-Y. Wei, Y.-S. Hsiao, J.-H. Huang, C.-Y. Hsu, F.-C. Chang, P. Chen, K.-C. Ho and C.-W. Chu, *RSC Adv.*, 2012, **2**, 4746–4753.
11 Z. Jiao, J. Wang, L. Ke, X. Liu, H. V. Demir, M. F. Yang and X. W. Sun, *Electrochim. Acta*, 2012, **63**, 153–160.
12 J. Zhang, J. Tu, X. Xia, Y. Qiao and Y. Lu, *Sol. Energy Mater. Sol. Cells*, 2009, **93**, 1840–1845.
13 H. Huang, J. Tian, W. Zhang, Y. Gan, X. Tao, X. Xia and J. Tu, *Electrochim. Acta*, 2011, **56**, 4281–4286.
14 S. Garreau, G. Louarn, J. Buisson, G. Froyer and S. Lefrant, *Macromolecules*, 1999, **32**, 6807–6812.
15 F. L. Souza, M. A. Aegerter and E. R. Leite, *Sol. Energy Mater. Sol. Cells*, 2007, **91**, 1825–1830.
16 E. M. Sorensen, S. J. Barry, H.-K. Jung, J. M. Rondinelli, J. T. Vaughey and K. R. Poeppelmeier, *Chem. Mater.*, 2006, **18**, 482–489.
17 L. Liang, J. Zhang, Y. Zhou, J. Xie, X. Zhang, M. Guan, B. Pan and Y. Xie, *Sci. Rep.*, 2013, **3**, 1936.
18 Z. Jiao, X. W. Sun, J. Wang, L. Ke and H. V. Demir, *J. Phys. D: Appl. Phys.*, 2010, **43**, 285501.
19 C. J. Hung, Y. H. Huang, C. H. Chen, P. Lin and T. Y. Tseng, *IEEE Trans. Compon., Packag., Manuf. Technol.*, 2014, **4**, 831–839.
20 L. J. Ma, Y. X. Li, X. F. Yu, Q. B. Yang and C. H. Noh, *Sol. Energy Mater. Sol. Cells*, 2008, **92**, 1253–1259.

